

JIA Zhang, GUO Jing-pu, LU Ying,
WANG Xin-feng, CHEN Chin-ping, XU Jun,
WANG Xiao-nan, ZHU Meng, FENG Qing-rong

A Study on the Components of MgB₂ Thick Film Prepared via HPCVD

© Higher Education Press and Springer-Verlag 2006

Abstract Superconducting MgB₂ thick film has been prepared via hybrid physical–chemical vapor deposition method on Al₂O₃ (0001) substrate by using B₂H₆ and magnesium ingot as raw materials reacted from 730 to 830°C for 40 min under 20 to 30 kPa. Its thickness is about 40 μm. The MgB₂ thick film shows T_c (onset) = 39.0 K and T_c (0) = 37.2 K. X-ray diffraction pattern shows that the film grown along (101) direction has small amount of impurities of Mg and MgO. Scanning electron microscopy and energy dispersive X-ray spectroscopy indicated that these impurities existed indeed and were Mg rich. The MgO film was formed on the surface of the MgB₂ thick film to further protect the sample from oxidation. We presented a new mechanism for the formation of the thick film.

Keywords MgB₂ film, SEM image, EDX, X-ray diffraction pattern

PACS numbers 74.62.Bf, 74.70.Ad, 74.78.-w

1 Introduction

The new superconductor, MgB₂, has attracted people's interest in fabrication, basic superconducting properties, and applied potential since its discovery in 2001 [1]. Especially, latest developments, such as the successful deposition of high-quality MgB₂ film with upper critical

field (H_{c2}) as high as 50 T [2], encourage people to test its large-scale application. High-quality MgB₂ samples with critical current density exceeding the Nb and Nb₃Sn wires and tapes promise a large possibility to replace current primary superconducting materials Nb and Nb₃Sn. Various kinds of MgB₂ superconductors, such as bulk, tape, wire, thin film, thick film, and so on, have been fabricated via different techniques. Bulk sample can be synthesized directly by sintering the reactants of boron and magnesium or commercial MgB₂ powders at different temperatures and protected atmospheres. Wires and tapes can be prepared by using Powder in Tube (PIT) technique [3] or diffusion of Mg vapor to B fiber [4,5]. For MgB₂ thin and thick films, synthesis can be induced generally using two kinds of methods: one is via a “two-step” method [6–9], i.e., depositing B film first, then annealing in Mg vapor and obtaining the MgB₂ thin films finally. The other is by way of a “one-step” method [10–13], i.e., direct fabrication, such as chemical vapor deposition (CVD) and electrophoresis. Nowadays, the advanced MgB₂ thin films with $J_c \sim 10^7$ A/cm², $H_{c2}(0)_{\perp ab} \sim 34$ T and $H_{c2}(0)_{\parallel ab} \sim 50$ T, as well as the MgB₂ thick film samples on metal substrates, such as Ta, Mo, W, Fe, Cu, and stainless steel [5], have been prepared successfully [2]. Our group has fabricated MgB₂ thick films on sapphire single-crystal substrate recently [14], and detailed investigation into its components is very significant in preparing thick film samples with remarkable J_c and H_{c2} as well as in exploring a new method of MgB₂ wires and tapes.

We carried out the analysis to the morphology and component of MgB₂ thick-film samples grown on (001) sapphire substrate prepared via hybrid physical–chemical vapor deposition (HPCVD) in this paper. These results would give feasible reaction conditions to the *in situ* fabrication of MgB₂ thick films on metal substrates.

2 Method and equipment

Fabrication of MgB₂ thick films was based on HPCVD technique [13], and concerned substrate was sapphire

Translated from *Chinese Journal of Low Temperature Physics*, 2005, 27(1) (in Chinese)

JIA Zhang, GUO Jing-pu, LU Ying,
WANG Xin-feng, CHEN Chin-ping, XU Jun,
WANG Xiao-nan, ZHU Meng, FENG Qing-rong (✉)
School of Physics and State Key Laboratory of Artificial
Microstructure and Mesoscopic Physics,
Peking University,
Beijing 100871, China
E-mail: qrfeng@pku.edu.cn

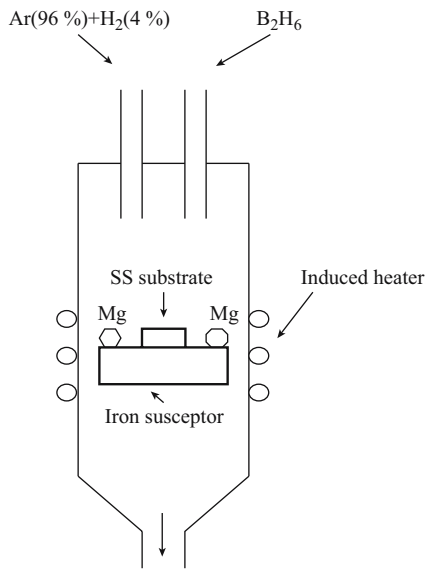
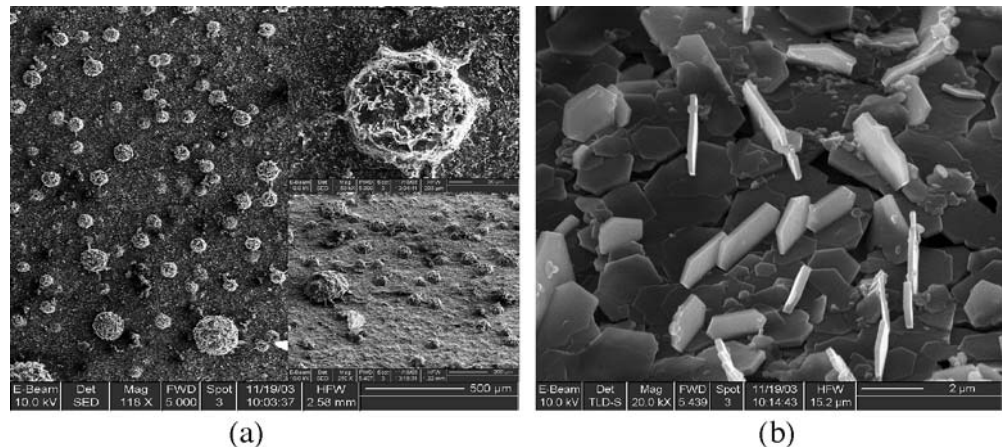


Fig. 1 Experiment set of HPCVD prepared for MgB_2 thick films on stainless steel substrate

single crystal with (0001) direction. Substrate was placed on the iron susceptor with 3–4 g Mg slugs around as source material. Susceptor was hung up and sealed in a vertical quartz tube reactor. A high-frequency inductive heater was fixed around the tube, as shown in Fig. 1. Carrier gas, which was a mixture of Ar (96%) and H_2 (4%), as well as another raw material, diborane (B_2H_6), was introduced into the reactor from a sealed pipe. The details were described elsewhere [14].

We investigated film surface morphology by using Stara BD325 FIB scanning electron microscopy (SEM). X-ray diffraction pattern was performed with Philips X'pert X-ray diffractometer. Surface study and component analysis were carried out via LEO 1450VP SEM and INCA ENERGY 300 energy dispersive X-ray spectroscopy (EDX), and the backscattering morphology was demonstrated via electron backscattering diffractometer (EBSD) equipped on channel 5 of this SEM.

Fig. 2 (a) SEM images of MgB_2 thick film magnified $\times 118$ using Stara BD325 FIB SEM. The *insert on the top right corner* was a bright granule magnified $\times 1\,500$, and the whole sample that was declined 45° was illustrated at the *bottom right corner*. (b) MgB_2 thick-film surface with a higher magnification ($\times 20\,000$)



3 Results and discussion

3.1 Analysis of experimental process

In the experimental process, we refused a complete steady temperature control and instead chose a particular method such that temperature was, at first, increased slowly, then in a rapid manner; after which, it was decreased manually and eventually maintained. We heated the iron susceptor inductively; 20 min later, thermocouples displayed an automatic and sharp increase in susceptor temperature from 730 to 830°C . Keeping this condition for 1 min, we manually and rapidly decreased the temperature to 700°C , which was maintained for 25 min. Then, we switched off diborane flow and cut heating power, which cooled down the samples to room temperature together with the reaction system. The temperature change during the whole process was described in [14].

Before the experiment, vacuum system was pumped under 100 Pa. Carrier gases, Ar (96%) and H_2 (4%), were introduced into the chamber slowly. During the whole reaction, these gases always kept flowing into the quartz tube at a pressure between 20 and 30 kPa.

3.2 Surface morphology

Figure 2(a) shows the surface image of MgB_2 thick film with a $\times 118$ magnification. We could see many bright granules with different dimensions on the rough sample surface. From the bottom insert, which was taken from the sample that was declined 52° , we could confirm that these grains were raised from the sample surface. Some granules almost parted from the sample surface completely, just like dropping on the surface. Others were rising from the surface but were still not separated from the surface. Upper insert was one of the grains with a $\times 1\,500$ magnification. We found that it was Mg rich via component analysis. As regards the formation of these grains, we considered that it was associated with the fabrication process; the details of which are described in the following processes.

1. At a certain time in the automatic temperature-rising period, formerly separated Mg ingots melted and

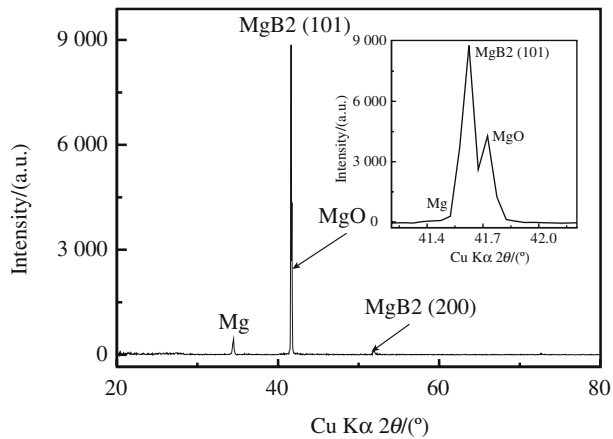


Fig. 3 XRD pattern of MgB₂ thick film on sapphire substrate prepared via HPCVD

connected to a whole part. This liquid Mg reacted fiercely with a boron atom decomposed from the continuous B₂H₆ flow and formed one MgB₂ layer above the surface of the melted Mg. However, this film was loose, inducing volatilized Mg from the bottom layer, which gushed through the film interspaces and shaped splitting morphology. These grains were linked to the film surface via many small MgB₂ crystallites, and the connections were as smooth as that of the whole part.

2. Continuous Mg vapor from the susceptor condensed to Mg grains in the temperature-rising process, including small amounts of MgB₂ crystallites. They dropped on the film surface and became granules. These granules only slightly stuck to the surface and not to the smooth connection; hence, there were no MgB₂ crystallite in the boundary. This was different from the former case.

Figure 2(b) shows another SEM picture with a $\times 20,000$ magnification of this thick-film sample. We could see that these thick films were composed of many sheet crystallites, where only narrow and no wide interspaces existed. Considering edge effect, the MgB₂ granule edges perpendicular to the film surface seemed bright, while the parallel ones obtained a dark color. From the figure, it can be deduced that most sheets of hexagonal MgB₂ granules deposited parallel to the film surface, not to mention small amounts of

Table 1 Element content ratio of B, O, and Mg studied via EDX from the six selected regions shown in the Fig. 4(a)

Element	Region					
	1	2	3	4	5	6
B	0	0	0	14.57	26.02	27.04
O	23.13	16.25	17.32	4.25	13.35	13.92
Mg	76.87	83.75	82.68	81.17	60.63	59.04

perpendicular ones. Component analysis revealed that the main elements constituting this thick film were boron and magnesium, with a small amount of oxygen in the film surface.

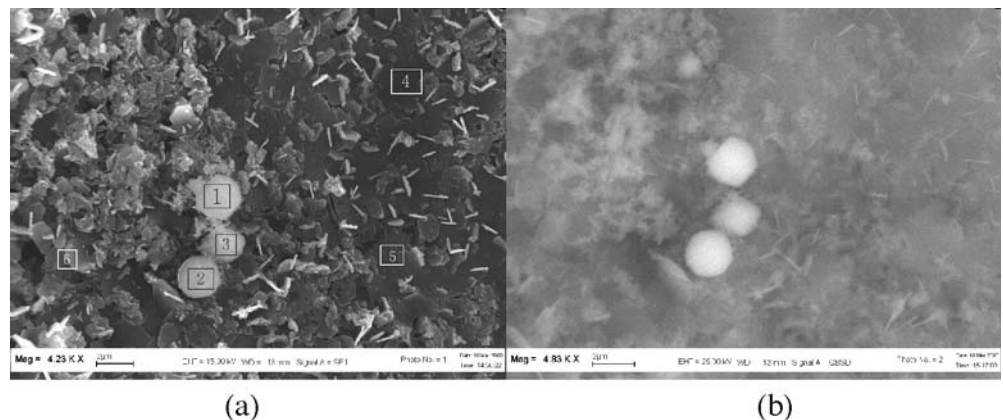
3.3 Quantitative analysis of components

X-ray diffraction pattern illustrated in Fig. 3 indicated that the most intensive peak was (101) of MgB₂; that is, this sample was well textured along the (101) direction. Other small diffraction peaks could be attributed to Mg and MgO impurities. Based on the measurement, we calculated the lattice constants $a = 3.192 \text{ \AA}$ and $c = 3.521 \text{ \AA}$, which were similar to the results of other groups. Then, we investigated elemental compositions in different areas via the EDX method.

From the SEM image exhibited in Fig. 4(a), which was $\times 4\,000$ magnified, we found that our thick-film surfaces were nonhomogeneous in structure. Component analysis was carried out to the six selected areas marked in the picture. Regions 1, 2, and 3 were bright, while regions 4, 5, and 6 were dark ones at different magnitudes. Setting the incident electron beam energy at 15 keV, we were able to obtain the contents of all elements, as shown in Table 1. As can be seen from this, regions 1, 2, and 3 were all composed of Mg or MgO because densities of Mg and MgO were higher than MgB₂, thus displaying a bright color in the observations, while regions 4, 5, and 6 consist of MgB₂ mainly. A small number of Mg and MgO for the Mg-rich results came from the data.

The reason we took 15 keV as incident energy was that EDX analysis provides accurate results to the light element boron within this energy extent. Although INCA

Fig. 4 (a) SEM image of MgB₂ thick film magnified $\times 4\,000$; the detailed composition information of six marked regions was investigated via EDX. (b) Backscattering image of MgB₂ thick film magnified $\times 4\,000$ in the same area as (a)



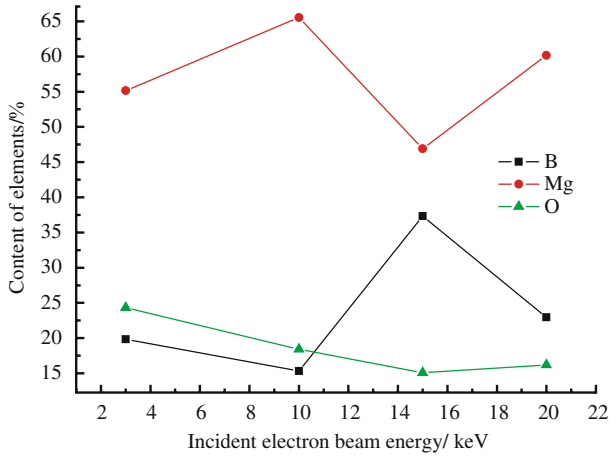


Fig. 5 Incident electron energy dependence of element content in a 0.06 mm² area

ENERGY300 EDX could obtain quantitative information to any element heavier than Be nominally, EDX technique was very imprecise in light-element measurement. Background noise affected measurement precision further, especially that of low-energy X-ray; hence, more corrections were needed in the data processing. A higher or lower incident electron energy would cause a failure in measuring light element or a false result. For heavy-element targets, we usually selected incident electron energy three to five times higher than the threshold value (i.e., binding energy); for light-element targets, incident electron energy was five to ten times higher than the threshold value [15]. However, it was not met in the practice. Binding energy of electron in K shell of boron was 188 eV, while it was 1 305 eV for magnesium; therefore, we could not decide an acceleration voltage to fit the needs of both boron and magnesium but could only resort to repeating the experiments. We focused the incident electron beam with different energies on a same region that has a size of about 0.06 mm² (Fig. 5). The results are shown in Table 2.

In the same region, the content of oxygen changed slightly, while both magnesium and boron had obvious deviations as the incident electron energy changed. From this, it follows that, for boron, when the electron energy of incident beam was about 15 keV, its K_{α} line was most intense. This maximum was restricted by two opposite factors: (1) X-ray intensity would increase as voltage increased; (2) when the energy of incident beam increased, X-ray would be generated in the deep part of the sample,

which increased the absorption for the meantime. Our results were consistent with electron energy dependence of B K_{α} intensity measured by Shiraiwa et al. in 1972 based on the investigation on several borides, such as FeB, Cr₅B₃, VB₂, and so on. The maximum of B K_{α} from their data all appeared in the range of 10–15 keV of electron energy [16]. Eyidi et al. [17] in Germany set the electron energy at 15 keV likewise when they carried out the analysis using the EDX technique.

Now, from the measurement and discussion above, we could confirm that bright areas did not contain boron but relative oxygen and magnesium, as can be seen in Fig. 4(b). The backscattering image of the same region proved this point as well as the existence of white floccules of MgO [18].

Theoretic calculation [19] and a large number of experiments [20–23] indicated that MgB₂ was very easy to be oxidated. In many fabrication processes, it is hard to prevent this oxidation from happening. As for our fabrication, oxygen was introduced mainly in the high-temperature period. It came from the residual atmosphere in the mixed gases (Ar and H₂) with purity 99.99%, impurity oxygen in Mg ingots, and oxygen adsorbed in the chamber wall. For example, in the sintering process for the preparation of MgB₂ bulk samples, samples were sealed with Ta slice. Regardless of the gases that flowed during sintering (purified argon or mixed argon and hydrogen), we could always find some degree of oxidation of Ta slice after the experiments as to where gases flowed into. On the other side of the Ta slice, no oxidation occurred or it was just very weak for it to be seen. This was because a small amount of oxygen was presented in the reducing gases, and oxidation will transpire (regardless of its extent) during the long period of sintering.

The report from Berenov et al. [23] claimed that impurity of MgO in MgB₂ would lower the transition temperature T_c . We thought that this conclusion was not exactly right. From a number of experiments, we found that our MgB₂ thick-film samples, using the HPCVD technique on sapphire substrate, had some MgO impurities but with no obvious decrease in T_c , which was still concentrated in the 38.7–39.4 K range. Therefore, the existence of MgO was not the direct reason for the decrease in T_c [7,24]. It was worth noticing that this HPCVD technique could prepare relatively dense samples [20], and our films were so thick that they could be classified as “quasibulk”. Bulk samples could maintain relatively high T_c all the time; thus, we

Table 2 Contents of three elements, B, O, and Mg, at different incident electron beam energies the marks of (1)–(3) in the column heading represented the order of three times of measurements

Elements	Electron beam energy / keV						
	3	10	15 (1)	15 (2)	15 (3)	20 (1)	20 (2)
B / %(atom)	20.06	15.57	35.74	35.44	41.48	32.72	13.67
O / %(atom)	24.54	18.66	16.84	14.20	14.93	14.48	18.33
Mg / %(atom)	55.40	65.77	47.42	50.36	43.60	52.80	68.00
			Average	Error		Average	Error
B			37.55	±2.78		23.20	9.53
O			15.32	±1.11		16.41	1.93
Mg			47.13	±2.77		60.40	7.60

deduced that films' compactness and good connection between granules guaranteed their high T_c . The existence of MgO and other impurities worsened these connections, thus finally lowering T_c .

As can be seen from the results of EDX, our films obtained a large amount of Mg. To the six selected areas, a rough estimation gave a Mg-to-B atom rate of 2:1, which was relatively high compared with the stoichiometric Mg/B value of 0.5. Even after considering a tiny amount of Mg(OH)₂ and MgCO₃ [25], the amount of Mg was still abundant. We considered that it was concerned with the deposition process: as described above, melted Mg reacted with B decomposed from B₂H₆ and formed one MgB₂ layer on surface; behind this layer, there was residual Mg, and above it, there were "dropped" Mg powder or granules. These Mg would form one layer of MgO as long as they contacted oxygen. Dramatically, this MgO thin layer could lower the oxidation inside of films [19]. From the EDX results to the cutting section of films, it demonstrated that the content of Oxygen atom was only about 4%. The content of Oxygen at the film surface was far larger than that at the center of the film and was not uniform.

Acknowledgements We thank Yan Xin for patient elemental composition analysis of EDX, and this study was supported by the Major State Basic Research Development Program of China (No. BKBRSF-G1999064602) and the Peking University President Fund.

References

- Nagamatsu J., Nakagawa N., Muranaka T., Zenitani Y. and Akimitsu J., *Nature*, 2001, 410: 63
- Gurevich A., Patnaik S., Braccini V., Kim K.-H., Mielke C., Song X., Cooley L.-D., Bu S.-D., Kim D.-M., Choi J.-H., Belenky L.-J., Giencke J., Lee M.-K., Tian W., Pan X.-Q., Siri A., Hellstrom E. E., Eom C. B. and Larbalestier D. C., *Supercond. Sci. Technol.*, 2004, 17: 278
- Glowacki B.-A., Majoros M., Vickers M., Evetts J.-E., Shi Y. and McDougall I., *Supercond. Sci. Technol.*, 2002, 14: 193
- Canfield P.-C., Finnemore D.-K., Budko S.-L., Ostenson J.-E., Lapertot G., Cunningham C.-E. and Petrovic C., *Phys. Rev. Lett.*, 2001, 86(11): 2423
- Feng Q.-R., Xu J., Guo J.-D., Wang X., Xiong G.-C., Gao Z.-X., Xu H.-Q., She D.-L., Cai S., Li Z.-Y. and Dong Y., *Chin. J. Low Temp. Phys.*, 2001, 24(2): 96
- Wang S.-F., Zhou Y.-L., Zhu Y.-B., Zhang Q., Liu Z., Chen Z.-H., Lu H.-B., Dai Y.-S. and Yang G.-Z., *Physica C*, 2003, 390: 6
- Eom C.-B., Lee M.-K., Choi J.-H., Belenky L.-J., Song X., Cooley L.-D., Naus M.-T., Patnaik S., Jiang J., Rikel M., Polyanskii A., Curevich A., Cai X.-Y., Bu S.-D., Babcook S.-E., Hellstrom E.-E., Larbalestier D.-C., Rogado N., Regan K.-A., Hayward M.-A., He T., Slusky J.-S., Inumaru K., Hass M.-K. and Cava R.-J., *Nature (Lond.)*, 2001, 411: 558
- Kang W.-N., Kim H.-J., Choi E.-M., Jung U.-C. and Lee S.-I., *Science*, 2001, 292: 1521
- Moon S.-H., Yun J.-H., Lee H.-N., Kye J.-I., Kim H.-G., Chung W. and Oh B., *Appl. Phys. Lett.*, 2001, 79: 2429
- Bu S.-D., Kim D.-M., Choi J.-H., Giencke J., Hellstrom E.-E., Larbalestier D.-C., Patnaik S., Cooley L., Eom C.-B., Lettieri J., Schlom D.-G., Tian W. and Pan X.-Q., *Appl. Phys. Lett.*, 2002, 81: 1851
- Liu Z.-K., Schlom D.-G., Li Q. and Xi X.-X., *Appl. Phys. Lett.*, 2001, 78: 3678
- Jo W., Huh J.-U., Ohnishi T., Marshall A.-F., Beasley M.-R. and Hammond R.-H., *Appl. Phys. Lett.*, 2002, 80: 3563
- Zeng X.-H., Pogrebnyakov A.-V., Kotcharov A., Jones J., Xi X.-X., Lysczek E., Redwing J.-M., Xu S., Li Q., Lettieri J., Schlom D.-G., Tian W., Pan X. and Liu Z.-K., *Nat. Matters*, 2002, 1: 35
- Liu Z.-B., Song X.-F., Wang Y.-Z. and Wang Z.-X., *Chin. J. Low Temp. Phys.*, 2003, 25: 71
- Pan C.-H. and Zhao L.-Z., *The Basic of Electron Energy Spectrum*, Beijing: Scientific Press, 1981, 59
- Shiraiwa T., Fujino N. and Murayama J. (eds.) In: *Proc. 6th Intl. Conf. on X-Ray Optics and Microanalysis*, Tokyo: Univ. Tokyo Press, 1972, 213
- Eyidi D., Eibl O., Wenzel T., Nickel K.-G., Schlachter S.-I. and Goldacker W., *Supercond. Sci. Technol.*, 2003, 16: 778-788
- Yang D.-L., Sun H.-W., Lu H.-X., Guo Y.-Q., Li X.-J. and Hu X., *Supercond. Sci. Technol.*, 2003, 16: 576-581
- Yan Y.-F. and Al-Jassim M.-M., *Phys. Rev., B*, 2003, 67: 212503
- Liao X.-Z., Serquis A.-C., Zhu Y.-T., Huang J.-Y., Peterson D.-E., Mueller F.-M. and Xu H.-F., *Appl. Phys. Lett.*, 2002, 80: 4398
- Klie R.-F., Idrobo J.-C., Browning N.-B., Serquis A., Zhu Y.-T., Liao X.-Z. and Mueller F.-M., *Appl. Phys. Lett.*, 2002, 80: 3970
- Zeng X.-H., Sukiasyan A., Xi X.-X., Hu Y.-F., Werta E., Tian W., Sun H.-P., Pan X.-Q., Lettieri J., Schlom D.-G., Brubaker C.-O., Liu Z.-K. and Li Q., *Appl. Phys. Lett.*, 2001, 79: 1840
- Berenov A., Lockman Z., Qi X., MacManus-Driscoll J.-L., Bugoslavsky Y., Cohen L.-F., Jo M.-H., Stelmashenko N.-A., Tsaneva V.-N., Kambara M., Hari Babu N., Cardwell D.-S. and Blamire M.-G., *Appl. Phys. Lett.*, 2002, 79: 4001
- Canfield P.-C., Finnemore D.-K., Bud'ko S.-L., Ostenson J.-E., Lapertot G., Cunningham C.-E. and Petrovic C., *Phys. Rev. Lett.*, 2001, 86: 2423
- Serquis A., Zhu Y.-T., Peterson D.-E., Mueller F.-M., Schulze R.-K., Nesterenko V.-F. and Indrakanti S.-S., *Appl. Phys. Lett.*, 2001, 80: 4401